

From bread waste to bacterial cellulose nanostructures: Development of a novel rotating disk bioreactor

Sotirios Pilafidis^a, Antiopi Vardaxi^a, Konstantina Kourmentza^b, Stergios Pispas^a,
Maria Dimopoulou^c, Erminta Tsouko^{a,d,*}

^a Theoretical and Physical Chemistry Institute, National Hellenic Research Foundation, 48 Vassileos Constantinou Ave., 11635 Athens, Greece

^b Department of Chemical & Environmental Engineering, Faculty of Engineering, University of Nottingham, University Park, NG7 2RD Nottingham, United Kingdom

^c Department of Wine, Vine and Beverage Sciences, School of Food Science, University of West Attica, Ag. Spyridonos str, Egaleo, 12243 Athens, Greece

^d Division of Genetics & Biotechnology, Department of Biology, National and Kapodistrian University of Athens, Zografou Campus, 15784 Athens, Greece

ARTICLE INFO

Keywords:

Bacterial nanocellulose
Bioreactor design
Renewable resources
Tunable properties
Bioprocess

ABSTRACT

A novel rotating disk bioreactor was designed and manufactured to produce bacterial cellulose (BC) using *Komagataeibacter rhaeticus*. Optimal conditions-45 % disk submersion, mechanically etched disks with rotation speed of 20 rpm, spacing of 35 mm and 0.5 vvm air supply- achieved a yield of 1020 mg BC/disk with commercial glucose. Bread waste enzymatic hydrolysates improved BC production by 133.3 %, highlighting the potential of waste valorization in sustainable biopolymer production. BC was further modified into nanostructures (BNCs) using H₂SO₄ (BNC1), H₂SO₄-HCl (BNC2), and cellulases (BNC3). FTIR spectra of BC and BNCs revealed typical cellulose vibration-bands while dynamic light scattering showed bimodal or trimodal size distributions (hydrodynamic radiuses of 60–2969 nm). TEM imaging of BNC1 and BNC2 demonstrated rodlike/needlelike nanostructure with widths of 33.1 ± 18.2 nm and 24.8 ± 14.2 nm respectively. BNC3 presented bundle of flat ribbons (width of 56.4 ± 26.3 nm). The maximum degradation temperature of BC (295 °C) decreased after its *ex-situ* modification (271–294 °C). The enhanced production and tailored structural modifications of BC highlight its potential for diverse applications in materials science. This transformative approach that integrates bread waste valorization and innovative bioreactor design paves the way for high-value advancements in biotechnology and environmental sustainability.

1. Introduction

Humanity is exerting irreversible changes on Earth, pushing the planet toward a critical threshold of biosphere integrity [1]. A 2020 study estimated that human-made mass, which has been doubling approximately every 20 years, now equals or even exceeds the total living biomass on Earth [2]. Identifying abundant, low-cost, and renewable agro-industrial side-streams to produce value-added products within the framework of a circular economy is a forward-looking strategy [3]. Since ancient times, bread has been the most widely consumed food item. Globally, over 100 million tons of bread are manufactured annually, while 129 million tons are consumed, with approximately 10 % of it being wasted throughout the manufacturing and consumption process. The management of bread waste (BW) presents considerable environmental and economic challenges worldwide,

and particularly in Europe, which accounts for 53.6 % of the global market share [4]. The disposal of BW, often through landfilling, contributes to greenhouse gas emissions, and thereby exacerbates climate change. Additionally, the energy, water, and raw materials used in bread production that end up as waste represent a considerable loss of resources. The economic burden is further intensified by the unrealized value of BW when it is not redirected for reuse or recycling. Given the vast scale of global bread production and consumption, these challenges are widespread highlighting the need for alternative solutions to ensure its sustainable management [5]. The favorable nutritional profile of BW, including starch (50–70 %), vitamins and other assimilable nutrients, enhances its suitability for microbial growth and makes it an ideal candidate for circular-oriented fermentation processes, where waste materials are bioconverted into value-added products such as enzymes, pigments, organic acids, and hydrogen [6,7].

* Corresponding author at: Theoretical and Physical Chemistry Institute, National Hellenic Research Foundation, 48 Vassileos Constantinou Ave., 11635 Athens, Greece.

E-mail address: etsouko@biol.uoa.gr (E. Tsouko).

<https://doi.org/10.1016/j.ijbiomac.2025.144374>

Received 22 January 2025; Received in revised form 12 May 2025; Accepted 17 May 2025

Available online 18 May 2025

0141-8130/© 2025 The Authors. Published by Elsevier B.V. This is an open access article under the CC BY license (<http://creativecommons.org/licenses/by/4.0/>).

Bacterial cellulose (BC) is an extracellular biopolymer mainly produced by *Acetobacter* bacteria. The main challenge for large-scale production of BC includes the prolonged fermentation time, low BC production rates, use of costly culture media and the lack of efficient bioreactor configurations. So far, the lab-scale production of BC involves mainly static or agitated fermentation mode in shake flasks with cellulose membrane being produced at the air-liquid interface [8]. Several bioreactor configurations such as rotating disk bioreactors (RDB), stirred-tank reactors, and airlift reactors have been reported for BC production [9]. Aeration and agitation are crucial since oxygen supply is directly related to the aerobic metabolism of *Gluconacetobacter xylinus*. Agitation rates higher than specific thresholds may lead to the formation of cellulose-negative mutants (Cel⁻) that shift the bacterial metabolism toward the formation of different by-products, i.e., acetan. Moreover, agitated systems may yield BC with a low crystallinity index, and inferior mechanical properties [10]. Stirred tank or airlift reactors may present challenges due to the hydrodynamic shear stress exerted on bacterial cells and adhesion of the culture broth to the walls and upper parts of the vessel [11,12]. Therefore, the development of robust bioreactors combined with efficient bacterial strains could support sustainable BC production.

Modification of BC (*in-situ* or *ex-situ*) is essential to customize its properties. Acid hydrolysis is widely used to produce micro/nano-fibrils and nanocrystals while enzymatic processes, although more environmentally friendly and milder, remain less commonly applied [13]. BC nanostructures (after modification) (BNCs) inherit multifunctional properties e.g., large specific surface area/reactivity, improved mechanical responsiveness, high crystallinity, biodegradability, biocompatibility, etc. These attributes make them suitable for applications in cutting-edge nanotechnological sectors like tissue engineering, drug delivery, and food packaging [14].

This study addresses a significant gap in the field of BC production by developing an RDB with tailored design features and specific operational parameters as an alternative to traditional fermentation systems. The proposed RDB incorporates a multi-level evaluation of variable disk-submersion levels, rotation speed, spacing, surface roughness, and air supply, to enhance fermentation control and overcome limitations of conventional static systems, such as poor mass transfer, inconsistent microbial adhesion, and inefficient process regulation. A second key focus of this study is the valorization of BW, which is an abundant and sustainable resource for BC production -an area not fully explored in previous studies. The use of effective BW-derived enzymatic hydrolysates as an alternative fermentation medium, could contribute to both food waste reduction and resource efficiency. Furthermore, this study extended its focus on BC modification (through acid- and enzymatic-assisted approaches) which holds significant relevance for tailored properties and scalability, improving its processability and expanding its use in advanced biotechnological applications. The BNCs were characterized in terms of morphology, chemical structure, thermal properties, surface charge, and size distribution. Overall, this study brings together innovations in bioprocess design, resource valorization, and material modification to advance sustainable BC production, unlocking its full potential across diverse applications.

2. Materials and methods

2.1. Raw material and microorganism

BW streams were sourced as defective items resulting from processing deficiencies and they were provided by the Stergiou Company (a Greek confectionery factory). Maintenance of the bacterial strain *Komagataeibacter rhaeticus* UNIWA AAK2 used for BC production and pre-culture preparation were performed according to Tsouko et al. [15].

2.2. Design, manufacture and operation of the novel RDB

The schematic diagram of the envisioned RDB is depicted in Fig. 1a. The bioreactor vessel (28 × 10 × 20 cm) was made from polymethyl methacrylate (Plexiglas) with a total volume of 5600 cm³ and a working volume of 2000 cm³. The shaft was a 3 mm diameter stainless-steel threaded rod. Polycarbonate disks, each with a 10 cm diameter and 3 mm thickness, were precision-cut using Computer Numerical Control (CNC) machining. The Plexiglas vessel was fitted on a wooden base facing an adjustable speed (1–50 rpm) 15 W geared motor (Aoutecan, China) connected to a rotating disk. This disk, fitted with four fixed samarium-cobalt magnets (15 mm diameter, 4.5 kg pull force each), transferred rotational motion from the motor to an internal disk within the sealed vessel through non-contact magnetic coupling, ensuring the shaft and attached disks rotated inside the vessel. To enable passive aeration, five 0.25 cm diameter holes were drilled in the vessel lid and covered with micropore tape. Active aeration was provided by an aquarium pump, delivering air at 0.5 vvm, with the air filtered through a 0.2 μm PTFE syringe filter before entering the sealed vessel. To ensure sterile conditions, the Plexiglas vessel was exposed to UV light inside a laminar flow hood cabinet for 20 min, while the stainless-steel shaft with the attached polycarbonate disks was autoclaved at 121 °C for 15 min. The sealed vessel was securely bound to the wooden base, ensuring that the magnets on the disk inside the vessel aligned in parallel with those on the disk connected to the motor. Finally, to maintain a stable temperature, the entire RDB system was placed inside an incubator.

2.3. Evaluation of RDB process parameters for BC production

The RDB process parameters to maximize BC production were investigated employing the one-variable-at-a-time method. Initially, different levels of disk submersion (25 %, 35 %, 45 %) into the fermentation broth were evaluated. The level of submersion area refers to the portion of the disk that is submerged in the liquid medium. The effective surface area of each disk was $2 \cdot \pi \cdot r^2$ corresponding to 39.2 cm², 76.9 cm², and 127.2 cm² for 25 %, 35 %, and 45 % disk submersion level, respectively. The effect of disk surface roughness was also examined, with both smooth polycarbonate disks and mechanically etched disks fixed simultaneously on the rotating shaft. Next, the study focused on the effect of different rotation speeds (5 rpm, 10 rpm, 20 rpm, and 25 rpm) on BC production. The impact of disk spacing was also evaluated by fixing eight to twenty disks on the shaft and adjusting the distance between them (10 mm, 20 mm, 30 mm, 35 mm). Subsequent experiments involved supplying air to the vessel at a rate of 0.5 vvm.

2.4. BW enzymatic hydrolyses

The BW was converted into a glucose-rich fermentation medium using commercial enzymatic formulations (thermostable α-amylases with an activity of 1300 U/mL and glucoamylases with an activity of 300 U/mL, both purchased from Novozyme, Denmark) to produce carbon sources and other micronutrients that can sustain BC production. BW slurries (pH adjusted to 5.5 with 5 M H₂SO₄) were initially treated with α-amylases for 1 h at 90 °C and 150 rpm. Afterward, the slurries were allowed to cool to 55 °C, and glucoamylases were added. Hydrolysis was carried out for 24 h under constant stirring at 150 rpm. At the end of the hydrolysis, the reaction was terminated by adding trichloroacetic acid, and the samples were centrifuged (9000 rpm, 20 min, at 5 °C). Reducing sugars (RS) that correspond to glucose were then determined.

Hydrolytic experiments were initially performed under different initial concentrations of dry BW (71, 142, 213 g/L) using 0.28 g α-amylase/100 g dry BW and 0.13 mL glucoamylase/100 g dry BW. Subsequently, enzymatic hydrolysis was evaluated under two additional enzyme dosages: i) 0.56 g α-amylase/100 g dry BW and 0.26 mL glucoamylase/100 g dry BW, and ii) 0.90 g α-amylase/100 g dry BW and

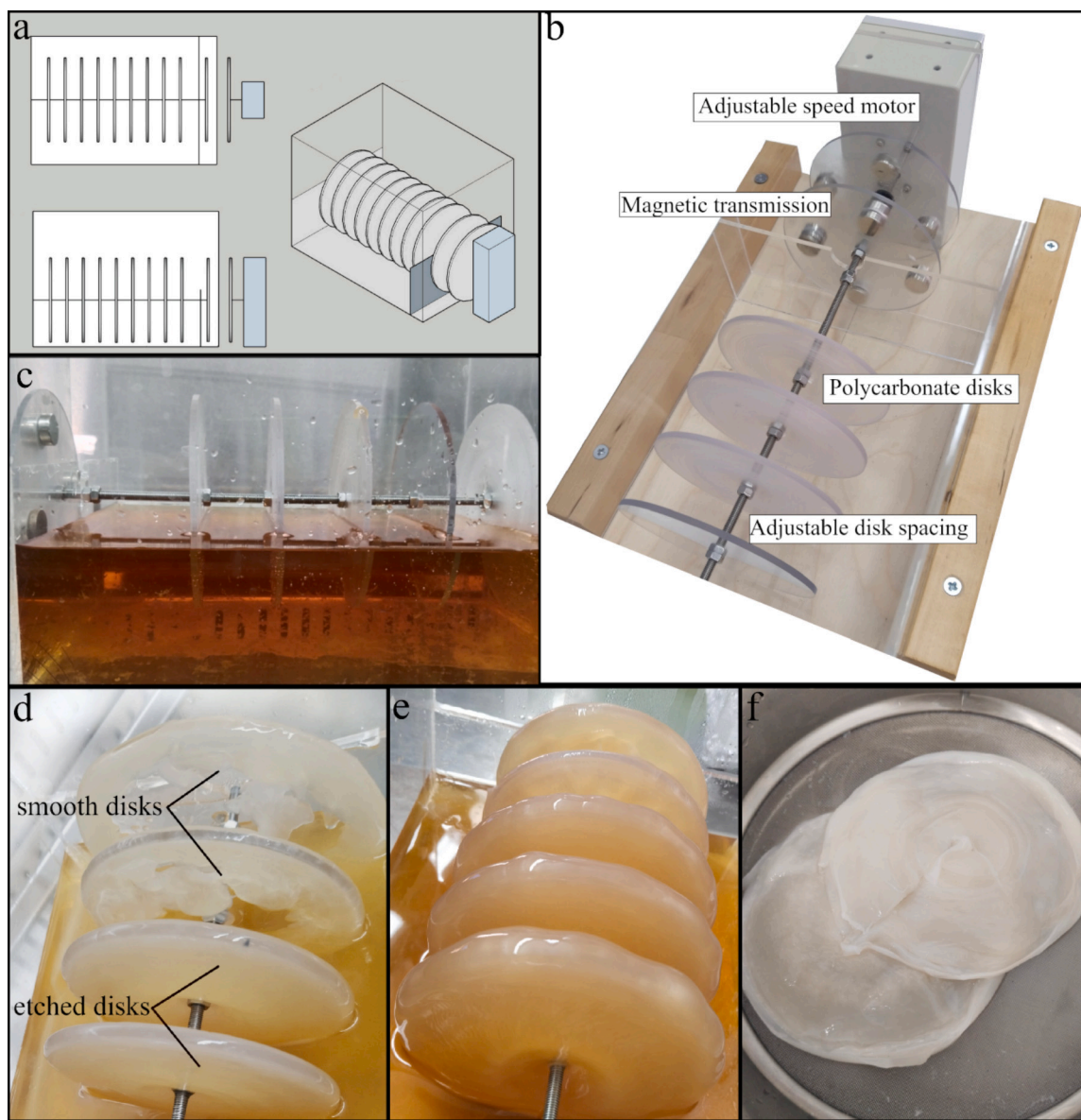


Fig. 1. Schematic diagram of top, front, and isometric view of the rotating disk bioreactor (RDB) design (a), configuration of the RDB (b), disks submerged in the fermentation media (c), weakly and partially attached bacterial cellulose (BC) on smooth disks and strongly attached BC fully covering the etched disks (d), BC attached to the RDB disks using bread waste enzymatic hydrolysates, before purification (e) and after purification (f).

0.45 mL glucoamylase/100 g dry BW. Enzymatic hydrolysates were centrifuged and filter-sterilized through a 0.22 μm filter unit (Polycap TMAS, Whatman Ltd.) prior to subsequent BC fermentations. Enzymatic hydrolysates were centrifuged and filter-sterilized through a 0.22 μm filter unit (Polycap TMAS, Whatman Ltd.) to be used in subsequent BC fermentations.

2.5. BC fermentation

Fermentations within the RDB were performed under batch mode, at 30 °C, using 10 % (v/v) of pre-culture and incubated for 7 days inside a static incubator. A solution of 5 M NaOH was used to maintain the pH of the media at a value of 6 ± 0.4 . The Hestrin and Schram medium (HS) [16] was employed throughout the experiments (in g/L: glucose 20, yeast extract 5, peptone 5, citric acid 1.15, and Na_2HPO_4 2.7). The best performing conditions were applied to a fermentation using BW enzymatic hydrolysates as the carbon source (20 g/L total sugars) simulated to the HS.

2.6. Ex-situ modification of BC

The acid-assisted hydrolyses of BC were carried out as described by Tsouko et al. [15]. Briefly, aqueous suspensions of lyophilized BC (produced from BW hydrolysates) (1.5 % w/v) were initially homogenized (IKA, ultra-turrax t 25 basic) for 4 min at 15,000 rpm. Hydrolyses were performed using appropriate acid amounts to reach 50 % (w/w) H_2SO_4 , and mixtures of 34.9 % (w/w) H_2SO_4 and 13 % (w/w) HCl. The hydrolyses conditions were 55 °C, 24 h and stirring at 500 rpm. The process was ceased using 5 mL of distilled water per 1 mL of BC aqueous suspension while 8 mL H_2O_2 (30 %) per 1 g dry BC was used for bleaching. The hydrolysates were centrifuged, rinsed twice with distilled water, and ultrasonicated (60 kHz, 300 W – Sonoplus 3200, Germany) for 5 min to eliminate the surplus acid. Finally, hydrolysates were centrifuged, and the precipitates (BNC1 for H_2SO_4 treatment and BNC2 for acid-mixture treatment) were transferred into dialysis membranes (Medicell Membranes Ltd., cut off Molecular weight 12–14 kDa) until a neutral pH was obtained and finally lyophilized.

Enzymatic-assisted hydrolysis of BC was carried out based on Rovera et al. [17] with slight modifications. BC aqueous dispersions (1 % w/v, pH = 5.5 fixed with 0.5 M HCl) were initially homogenized (4 min, 15,000 rpm) to facilitate enzyme access into the cellulose followed by sterilization (121 °C, 15 min) to avoid microbial contamination during the process. Subsequently, commercial cellulases from *Trichoderma reesei* (≥ 700 units/g, Sigma Aldrich) were aseptically added to BC suspensions (50 U/g BC). The enzymatic hydrolysis was performed at 55 °C, and 500 rpm. After 24 h of hydrolysis, slurries were centrifuged, followed by repeated washing steps with distilled water to remove enzymes and finally lyophilized (BNC3).

2.7. Characterization of BC and BNCs

The water holding capacity (WHC) of BC was measured based on the protocol of Natsia et al. [18]. Briefly, the BC membranes were shaken twice to remove surplus water, and then they were weighed. Complete removal of water from BC samples was achieved after drying at 40 °C for 48 h. The WHC was calculated as follows:

$$WHC = \frac{W_{wet} - W_{dry}}{W_{dry}} \quad (1)$$

where W_{wet} is the weight (g) of BC before drying and W_{dry} is the weight (g) of BC after drying.

Transmission electron microscopy (TEM) was used to observe the surface morphology obtained after each BC treatment. The images were scanned by JEOL 2100Plus high-resolution TEM equipped with a Gatan OneView IS Camera operating at an accelerating voltage of 200 kV. Fiber diameters were measured using ImageJ software by analyzing 50 individual fibers per TEM image to ensure statistical reliability. A water suspension (0.1 % w/v) was prepared and a 3 μ l drop was deposited onto carbon support film TEM continuous carbon grid (EMResolutions) and allowed to dry, while no staining was applied.

Dynamic light scattering (DLS) measurements were conducted using an ALV system (ALV-CG-3 goniometer/ALV-5000/EPP multi tau digital correlator) equipped with a He–Ne laser ($\lambda = 632.8$ nm). The field autocorrelation functions were analyzed utilizing the CONTIN algorithm, and relaxation rate distributions were extracted. The Stokes-Einstein relation was used to determine the hydrodynamic radius (R_h) distributions.

ζ -Potential measurements were conducted using a Zetasizer Nano ZS (Malvern Instruments, Worcestershire, UK) at 25 °C. Henry equation under the Smoluchowski approximation was used to calculate ζ -potential from the measured electrophoretic mobility. The results are presented as averages over 50 scans made at scattering angle $\theta = 173^\circ$. The DLS and ζ -potential were measured in suspensions of 0.1 % w/v lyophilized samples that were previously diluted with deionized water to avoid multiple scattering effects.

Attenuated total reflectance (ATR) Fourier Transform infrared spectroscopy (FTIR) measurements were performed on a Bruker Equinox 55 instrument equipped with an ATR diamond accessory from SENS-IR and a press. The samples were measured in the wavenumber range of 525–5000 cm^{-1} performing 64 scans at 2 cm^{-1} resolution.

Thermogravimetric analysis (TGA) of BC and hydrolyzed BC was performed at a TGA Q500 analysis System (TA Instruments) employing a nitrogen flow of 50 mL/min. Samples were precisely weighed (5–10 mg) into a TGA cup and heated under nitrogen flow to avoid oxidation. Sequentially, the temperature increased to 800 °C at a rate of 10 K/min.

2.8. Analytical methods

The determination of total RS was carried out using the 3,5-dinitrosalicylic acid (DNS) method [19] expressed as glucose equivalents. Free amino nitrogen (FAN) was determined using the ninhydrin method [20]. Starch quantification was performed enzymatically using the total

starch assay kit (K-TSHK, Megazyme, Ireland) which is based on AOAC Method 996.11 and AACC Method 76.13.01 [21,22].

The BC membranes obtained after each fermentation were purified as follows: BC samples were immersed in 0.1 M NaOH and boiled for 30 min. Subsequent washing steps were performed until a neutral pH was achieved. BC was dried at 40 °C until a constant weight and the dry weight was reported as BC concentration in g/L.

2.9. Statistical analysis

The statistical analysis was performed using R Studio (version 2024.04.2 + 764). ANOVA was conducted to assess differences between groups. Significant differences between means were determined by Honest Significant Difference (HSD-Tukey test) ($p < 0.05$). Data were reported as mean values \pm standard deviation of three independent replicates.

3. Results and discussion

3.1. Configuration of the novel RDB

The design of the RDB was inspired by prior research conducted in this field, aiming to provide transparency in the manufacturing and operation aspects. In this context, a bench-scale RDB was constructed to provide a straightforward, and user-friendly solution to facilitate the scaling-up potential of BC production (Fig. 1b). The RDB developed in this study was inspired by the well-established concept of rotating biological contactors (RBC), whose scalability has been explored in wastewater treatment applications [23]. The modular design, high interfacial area, low maintenance costs, and operational simplicity of RBCs support their adaptation to larger-scale bioprocesses [24], offering a foundation for scaling the RDB. Possible scale-up strategies include increasing shaft length and/or disk diameter to proportionally expand the surface area available for BC production. Alternatively, multiple RDB units can be operated in parallel, as demonstrated in other rotating disk systems such as the rotating disk bioelectrochemical reactor, where production capacity was enhanced through modular elongation and disk addition [25]. Furthermore, optimizing key scale-dependent factors—including oxygen transfer rate (kLa), and shear stress, which have been extensively studied in RBC systems—could offer a feasible direction for scaling the RDB [26]. For instance, oxygen transfer can be influenced by both the rotational speed and diameter of the disks, which can be adjusted to maintain adequate oxygenation in scaled-up systems. Additionally, computational modeling and pilot-scale testing could also support the identification of design features that promote uniform mixing and minimize the risk of dead zones during scale-up [27]. Also, the power input per volume (P/V) needs to be carefully considered to balance energy use with adequate agitation and favorable productivity [28]. Mechanical aspects, including shaft stability and disk dimensions, may also require attention to avoid excessive angular velocities at the disk edges—concerns consistent with general principles of bioreactor engineering and already explored in related systems [29].

A key design feature of the RDB is its modular shaft, which enables targeted adjustment of disk spacing using stainless steel nuts (Fig. 1b). This flexibility allows for the optimization of microbial adhesion, BC accumulation, and mass transfer efficiency by fine-tuning the distance between disks, based on process requirements. Additionally, the shaft design ensures controlled submersion of the disks into the fermentation medium (Fig. 1c), a critical parameter influencing oxygen transfer and nutrient availability. Unlike conventional RDBs with fixed disk arrangements, this adjustable configuration enhances process adaptability, making it suitable for optimizing bioprocess conditions [30,31]. The disks were either left untreated, maintaining a smooth surface, or they were mechanically etched using sandpaper to increase surface roughness, thereby enhancing their adhesive potential.

The main novelty of the RDB is that the mechanical force required for

disk rotation inside the vessel was transferred indirectly using magnetic coupling. More specifically, a set of external drive magnets was coupled to a set of driven magnets inside the vessel. The drive magnets were fixed on the external disk which was rotated by an electric motor at the desired speed transmitting rotation force to the coupled driven magnets inside the RDB sealed vessel (Fig. 1b). The use of magnetic coupling in the RDB minimizes contamination risks, as it eliminates the need for mechanical seals that are prone to wear and leakage. However, potential limitations of this approach are closely related to reduced transmission efficiency in highly viscous environments and long-term durability of the magnetic components. In high-viscosity media, torque transmission efficiency can be improved by optimizing magnetic coupling configuration (e.g., shape, size, and arrangement of magnets) to enhance magnetic flux and reduce slippage. Additionally, selecting high-performance materials for the containment shell, such as polyetheretherketone or advanced ceramics, can minimize friction and heat generation. Rare-earth magnets, which are commonly used for high magnetic strength, are susceptible to corrosion and demagnetization over time. To mitigate this, protective coatings such as polytetrafluoroethylene, epoxy resins, or corrosion-resistant alloys like Hastelloy-C can be applied, thereby extending operational lifespan and maintaining performance [32,33]. In scenarios where higher torque or operation under extreme viscosity is required, electromagnetic coupling systems may present a promising alternative. Unlike permanent magnets, electromagnetic couplings allow for dynamic control of torque via modulation of the electromagnetic field, enhancing performance under variable load conditions and reducing the risk of slippage [34]. However

it is important to note that electromagnetic systems may introduce heat generation, additional power input, and electromagnetic interference [35].

While magnetic-driven agitation is increasingly used in bioreactors designed for highly sterile processes, its integration into an RDB for BC production has not been reported in detail in the literature [30,36]. Most studies utilizing RDBs either omit descriptions of the rotation mechanism or rely on conventional shaft-driven systems with closed-type lip seals or transmission bearings, which pose sterility concerns due to potential leakage or contamination through moving parts [37,38]. Additionally, while some publications mention the use of closed-type lip seals and transmission bearings, they do not provide specific details on the transmission mechanism employed which may affect sterility [39–41]. Our approach ensures an effective sealed design that minimizes contamination risks and improves bioprocess control. This design is particularly beneficial for microbial culture applications, especially when higher levels of sterility are required [36]. Although BC fermentation does not demand highly sterile conditions, this approach could significantly benefit microbial co-cultures, such as those involving BC-producing bacteria and engineered microorganisms, which are used to produce novel BC composites for biomedical applications [42].

The vessel of the RDB was constructed out of plexiglas to allow for the visual inspection of the fermentation and the disks were CNC-cut out of polycarbonate. High-grade polycarbonate is a material which can withstand heating up to 140 °C, making it suitable for autoclaving. The material used to manufacture the disks in rotating biological contactors is a critical factor since it should properly accommodate the microbial

Table 1

Effect of disk surface texture and submersion level, rotation speed, distance between disks, and air supply on bacterial cellulose production and thickness per disk, glucose and free amino nitrogen consumption, and water holding capacity of the produced bacterial cellulose using the RDB.

Fermentation media	Conditions and configuration	Variable	BC/disk (mg)	BC thickness (mm)	Glu cons (% w/w)	FAN cons (% w/w)	WHC (w/w)
Glucose-based	Effect of disk area submerged, and disk surface texture	Disk area submerged (%)					
		25	101.1 ± 3.9 ^d	4.8 ± 0.3 ^c	32.1 ± 1.9 ^d	50.5 ± 5.3 ^c	97.4 ± 8.1 ^a
	Smooth disks, 5 rpm, no aeration	35	132.0 ± 6.6 ^c	7.9 ± 0.3 ^b	37.3 ± 2.6 ^c	53.7 ± 3.2 ^b	98.2 ± 5.6 ^a
		45	180.2 ± 5.7 ^b	8.1 ± 0.5 ^b	48.2 ± 4.8 ^b	55.6 ± 3.6 ^a	100.3 ± 5.2 ^a
		45	220.5 ± 7.6 ^a	9.1 ± 0.1 ^a	50.9 ± 2.5 ^a	55.1 ± 2.7 ^a	98.6 ± 12.3 ^a
Glucose-based	Effect of disk rotation speed	Rotation speed (rpm)					
		5	220.0 ± 7.6 ^c	9.1 ± 0.4 ^c	50.9 ± 2.5 ^b	57.1 ± 2.7 ^b	98.6 ± 12.3 ^a
	Etched disks, 45 % disk submersion, no aeration	10	353.6 ± 30.1 ^b	9.9 ± 0.3 ^b	55.8 ± 7.8 ^b	59.1 ± 2.5 ^{ab}	99.4 ± 8.8 ^a
		20	442.7 ± 29.4 ^a	13.7 ± 0.7 ^a	62.4 ± 8.9 ^a	61.6 ± 3.1 ^a	90.1 ± 2.1 ^b
		25	445.4 ± 28.3 ^a	14.3 ± 0.6 ^a	61.5 ± 6.6 ^a	60.8 ± 5.2 ^a	77.9 ± 0.7 ^c
Effect of disk spacing and aeration	Disk spacing (mm)						
	10	442.2 ± 29.4 ^c	13.7 ± 0.6 ^b	62.4 ± 8.9 ^b	61.6 ± 3.1 ^a	90.1 ± 2.1 ^{ab}	
Glucose-based	Etched disks, 45 % disk area submersion, 20 rpm, no aeration	20	470.6 ± 20.7 ^c	18.9 ± 1.5 ^b	66.6 ± 7.1 ^b	63.9 ± 2.6 ^a	92.3 ± 4.6 ^{ab}
		30	560.3 ± 22.6 ^b	29.9 ± 1.5 ^a	75.9 ± 3.6 ^a	64.7 ± 6.5 ^a	91.7 ± 2.8 ^b
		35	611.5 ± 57.2 ^a	33.3 ± 1.3 ^a	78.6 ± 9.8 ^a	65.2 ± 4.5 ^a	99.1 ± 5.6 ^a
		40	602.3 ± 51.7 ^{ab}	31.4 ± 0.9 ^a	76.2 ± 7.4 ^a	63.6 ± 7.2 ^a	94.2 ± 7.4 ^{ab}
Glucose-based	Etched disks, 45 % disk submersion, 20 rpm, aerated (0.5 vvm)	35	1020 ± 87.2 ^b	34.3 ± 0.8 ^a	80.1 ± 3.2 ^a	68.2 ± 1.5 ^a	108.8 ± 4.3 ^a
BW hydrolysates	Etched disks, 45 % disk submersion, 20 rpm, aerated (0.5 vvm)	35	2380 ± 0.4 ^a	31.2 ± 1.6 ^b	69.4 ± 2.1 ^b	69.5 ± 1.3 ^a	53.2 ± 4.8 ^b

WHC: water holding capacity in g water/g dry BC; BC: bacterial cellulose; Glu: glucose; FAN: free amino nitrogen; cons: consumption; BW: bread waste. Different superscript letters within same column, with the same conditions, indicate statistically significant differences ($p < 0.05$). In the case of BW-hydrolysates, the superscripts indicate statistically significant differences compared to the glucose-based medium under the same optimal conditions.

adherence, accumulation of BC while being durable, and able to withstand autoclaving or disinfection. Materials such as polypropylene, polyethylene, plexiglas, stainless steel, and even 3D-printed polycarbonate disks have been used in BC fermentation systems [39–41].

3.2. Effect of disk submersion level and disk surface roughness on BC production

Initial experiments showed that different levels of disk submersion into the fermentation significantly affected BC production ($p < 0.05$) when smooth disks were used. Increasing the submersion levels led to increased BC synthesis and accumulation (Table 1) with the highest BC production (180 mg BC/disk) being achieved when 45 % (157 cm² effective area) of the disk was submerged. In this study, submersion levels higher than 45 % were not evaluated since it would expose the rotating shaft to the liquid medium and possibly result in damage and rotation collision [43]. In all cases, the WHC of the produced BC was >97 g water/g dry BC. The consumption of FAN and RS varied between 50–56 % and 32–48 % respectively after 7 days of fermentation (Table 1).

Increasing the level of submersion area (up to a specific threshold) is positively correlated to oxygen availability and nutrient diffusion, promoting BC synthesis [24]. Submersion levels of 50 % have been reported to promote bacterial growth in a RDB. When submersion depth exceeded 50 %, BC production was hindered presumably due to decreased oxygen diffusion [43]. Soleimani et al. [31] used an RDB system with fixed disk surface submersion at 43.5 % and reported the production of 620 mg BC/disk at 8 rpm. In another study, 680 mg BC/disk was achieved using a RDB similar to the present one, at a constant disk submersion level of 34 % and 1 L of medium [40].

In the aforementioned experiments, it was observed that BC did not adhere homogeneously to the smooth surface of the disks (Fig. 1d). To overcome this obstacle, the effect of the disk surface roughness was investigated. More specifically, the surface of the disks was mechanically etched using sandpaper, resulting in a consistent rough texture. Under the optimal disk submersion level (45 %), and using etched disks, BC production was significantly enhanced ($p < 0.05$) compared to fermentation that involved smooth disks. The rougher surface creates a more favorable environment for bacterial growth and BC deposition, as the bacteria can adhere more firmly, leading to increased BC yield. Sharma et al. [41] conducted fermentations using smooth stainless-steel disks with holes with 16 mesh size. They remarked that mesh size is a critical factor for attachment since small mesh disks facilitated the attachment of BC on the disks and resulted in the maximum amount of BC/disk. A very interesting study from Lin et al. [37] showed that composite disks made of 50 % polypropylene and other ingredients such as soybean hulls, flour and yeast extract were effective for BC attachment and production (0.34 g/L/day). The incorporation of nutrient sources in the disks allowed bacteria to grow on the disk and eliminated the need for reinoculation, achieving semi-continuous conditions (five consecutive runs). In another publication, the comparison between plexiglas and four different polyethylene disks (integrated, perforated, lace covered, and stainless steel covered) revealed that integrated polyethylene was better suited leading to 0.74 g BC/disk [31].

3.3. Effect of disk rotation speed on BC production

The optimal rotation disk speed should be one to two times the disk radius, though some studies suggest that speeds up to five times the radius can also be beneficial [31,43]. Being in line with these reports, and considering that the disk radius was 5 cm, four distinct rotation speeds were evaluated, ranging from an initial 5 rpm to a maximum of 25 rpm (Table 1). In all cases, RS and FAN consumption ranged between 50.9 and 62.4 % and 57.1–61.6 % respectively in all cases. WHC of the produced BC was inversely related to the rotation speed when applying 10–25 rpm. Studies have shown that shear stress from increased

agitation, may disrupt the alignment and aggregation (linked to porosity) of cellulose chains, leading to denser and more compact structures with reduced WHC [10,44].

In this study, increasing the speed rotation up to 20 rpm led to a substantial increase in BC production indicating an optimal balance between oxygen transfer, shear stress tolerance, and stable bacterial adhesion in the given RDB configuration. Further rise did not affect the produced BC/disk. Moderate shear stress improves oxygen transfer and nutrient distribution within the fermentation media, supporting the aerobic metabolism of BC-producing bacteria. However, excessive rotational speeds can cause over-aeration, elevating dissolved oxygen levels and shifting metabolism toward gluconic acid production—an alternative pathway that competes with BC synthesis [45,46]. Moreover, shear stress generated from agitation may promote genetic instability, increasing the risk of spontaneous mutations from cellulose-producing (Cel⁺) to cellulose-negative (Cel⁻) mutants. This is attributed to the disruption of bacterial membranes and interruption of the cellulose polymerization process [46–48]. To add, excessive shear stress -exerted on bacteria adhered to the disks- has been associated with cell detachment, reduced bacterial adhesion, and lower enzymatic activity required for cellulose polymerization [10].

Reported optimal rotation speeds in RDB span 2–35 rpm; however, results remain inconsistent due to variations in the RDB design [49]. For instance, an RDB system (4000 cm³, 8 disks, 2.5 L active volume) produced 5 g/L BC at 7 rpm using *Gluconacetobacter xylinus* NCIM 2526, while increasing the rotation speed to 9 or 12 rpm significantly reduced BC yields due to excessive aeration [41]. Similarly, *Acetobacter xylinum* 0416 produced maximum BC at 7 rpm (active volume = 4 L), while a slight increase of the rotation led to reduced yields [50]. In contrast, other studies reported higher optimal speeds, such as 15 rpm (yielding 5.4 g/L BC) using *Gluconacetobacter* sp. RKY5 in an 8-disk RDB system (1-L active volume, 4-day fermentation) [40] and 13 rpm (yielding 900 mg BC/disk) using *Acetobacter xylinum* PTCC 1734 in a 3-L (active volume) bioreactor [31].

3.4. Effect of disk spacing and air supply

Subsequent experiments evaluated disk spacing ranging from 10 to 35 mm to maximize BC production. Disk spacing up to 20 mm did not significantly enhance BC production. Stepwise increase of disk spacing to 30 and 35 mm resulted in a 1.3-fold and 1.4-fold increase of BC/disk compared to the default spacing of 10 mm. The highest BC production of 611 mg BC/disk accompanied by the maximum BC thickness (33.3 mm) and WHC (99.1 g water/g dry BC) were obtained at 35 mm disk spacing while further increase of the spacing did not show any significant contribution ($p < 0.05$) to BC production. Increased disk spacing led to increased consumption of RS (62.4–78.6 %) and FAN (61.6–65.2 %). Insufficient spacing between disks may impede nutrient diffusion, resulting in localized nutrient depletion around the disks, potentially inhibiting bacterial growth and BC synthesis. Optimal disk spacing can minimize the competition among neighboring colonies for space and nutrients [10,51]. In the study of Soleimani et al. [31] the disk spacing of 20 mm resulted in the highest production of BC equal to 900 mg/disk, while further increase of the distance was to the detriment of BC synthesis. Increasing the disk spacing corresponds to less disks mounted on the shaft, which could mean less overall BC production. Nevertheless, this study presents a bioreactor prototype and highlights the key factors influencing BC production. Once key factors affecting BC production are identified, a new vessel with the appropriate length to accommodate more disks can be used with the same motor, optimizing the relationship between the number of disks, BC/disk, and overall BC production.

The implementation of aeration in the RDB led to a 67 % increase in the amount of BC/disk, as compared to the fermentation that air supply was not provided. BC thickness was also favored reaching 34.3 mm while RS and FAN consumption were slightly increased. The air supply had a beneficial impact on the WHC (108.8 g water/g dry BC) of BC.

Aeration has been correlated with structural changes in the arrangement of BC nanofibrils [44,52] probably leading to larger pore sizes of BC and thus greater amounts of water being trapped within the BC matrix. The beneficial effect of aeration on BC production was also reported by Soleimani et al. [31] who concluded that under a constant aeration rate of 0.5 vvm in a RDB, BC production was improved by 64 % compared to the non-aerated process. In another study, increasing the aeration rate to 1.25 vvm yielded the highest BC production levels, while further increase had a detrimental effect on BC biosynthesis [29]. Other studies that employed RDB did not incorporate supplemental aeration in the fermentation vessel, and instead used passive aeration [37,39,41,53]. Air sparging of 0.25 vvm has been suggested as favorable for BC production (11.6 g/L) when fermentations were performed in tray bioreactors using free sugars derived from orange peels and *K. sucrofermentans* [54].

Oxygen availability enhances BC biosynthesis by sustaining aerobic respiration, which generates ATP via oxidative phosphorylation to drive energy-intensive processes. In this metabolic framework, hexoses (e.g., glucose) are metabolized via the pentose phosphate pathway to produce UDP-glucose (the direct precursor of cellulose), while three-carbon compounds (e.g., pyruvate) and carboxylic acids enter gluconeogenesis coupled with the tricarboxylic acid cycle, producing intermediates that are channeled into UDP-glucose synthesis. ATP powers (i) UDP-glucose synthesis through phosphorylation and uridylyltransferase activity, and (ii) the *bcs* operon-encoded cellulose synthase complex (BcsA/BcsB), which polymerizes UDP-glucose into β -1,4-glucan chains. *BcsC* and *BcsD* mediate fibril extrusion (through transmembrane pores) and hierarchical fibril assembly into crystalline ribbons [46,55]. Consequently, increased ATP yield via oxygen availability ensures sufficient energy for precursor synthesis and polymerization/extrusion processes, directly relating oxygen availability with BC yield [56]. However, excessive oxygen levels beyond a certain threshold may shift metabolic priorities leading to reduced BC yields. For example, excessive oxygen can induce oxidative stress in bacterial cells, damaging cellular components and disrupting metabolic pathways essential for BC production. Moreover, cell growth over BC synthesis may be favored by redirecting cellular resources toward biomass formation [57–59].

3.5. Characterization of BW and production of enzymatic hydrolysates

The BW used in this study were defective items that failed to meet the quality control standards during their preparation process. These discarded products, typically deemed unsuitable for consumer consumption, represent a valuable yet underutilized resource. BW consisted predominantly of starch (60.9 ± 3.0 % w/w), soluble sugars (13.2 ± 3.6 g/L) and oil (8.9 ± 0.6 % w/w) while ash content was 1.45 ± 0.1 % (w/w). BW exhibited a pH value of 7.5 ± 0.3 , and a moisture content of 29.1 ± 1.4 % (w/w). The range of starch content in bakery waste is reported to fall between 50 % and 70 %, with water content ranging from 25 % to 35 %. The pH level of this waste is typically found to be between 4.0 and 7.0, while its ash content ranges from 1 % to 4 %. Bakery waste is known to have a lipid content of 1 % to 3 %. It is important to note that these values are based on reported averages and may vary depending on the specific product, bakery and production processes used [4,5,60].

Initially, several concentrations of BW (71, 142, 213 g/L) were subjected to enzymatic hydrolysis using commercial α -amylases (0.28 g/100 g dry BW) and glucoamylases (0.13 mL/100 g dry BW) (Table 2). Hydrolysis at 142 g/L BW showed the highest starch to glucose conversion yield ($Y_{S/Glu}$) equal to 53.8 % while the $Y_{S/RS}$ drastically decreased when initial BW concentration was 71 g/L or 213 g/L.

The effect of several enzyme dosages was also evaluated to maximize the $Y_{S/RS}$ (Table 2). Elevated α -amylase and glucoamylase activity led to increased RS production and $Y_{S/RS}$ that reached respectively 60.2 g/L and 66.2 % when α -amylase of 0.90 g/100 g dry RSW and glucoamylase of 0.45 g/100 g dry RSW were applied. The most commonly applied techniques for BW saccharification involve the use of acid treatment and

Table 2

Enzymatic hydrolysis of bread waste using commercial enzymes at three initial concentrations of solids (71, 142, 213 g/L) and different concentrations of enzymes after 24 h.

BW concentration (g/L)	α -Amylase (g/100 g BW)	Glucoamylase (mL/100 g BW)	Glucose produced (g/L)	$Y_{S/Glu}$ (%)
71	0.28	0.13	16.1 ± 0.4^d	33.9 ^d
142	0.28	0.13	48.9 ± 1.2^b	53.8 ^c
213	0.28	0.13	47.1 ± 0.6^c	32.9 ^d
142	0.56	0.26	50.5 ± 0.8^b	55.6 ^b
142	0.90	0.45	60.2 ± 1.7^a	66.2 ^a

BW: bread waste; $Y_{S/Glu}$: yield of starch conversion to glucose.

Different superscript letters within same column indicate statistically significant differences ($p < 0.05$).

enzymatic hydrolysis. Zhang et al. [60] reported that enzymatic hydrolysis of 30 % w/v bread, cake, and pastry waste produced 104.8, 35.6, and 54.2 g/L glucose, respectively. Similarly, Sigüenza-Andrés et al. [61] used a 25 % w/v solid BW and achieved 126.9 g/L glucose production. Another study reports an impressive 86 % glucose conversion yield from BW when enzymatic hydrolysis conditions were optimized [62]. Crude enzyme consortia produced in solid state fermentation by *Aspergillus awamori* provided efficient saccharification for confectionery waste streams leading to the production of 112.4 g/L total sugars [14].

3.6. Effect of BW enzymatic hydrolysates on BC production

The best performed conditions of the novel RDB were applied in fermentations that involved the use of BW-based enzymatic hydrolysates. BW-derived hydrolysates supported efficient bacterial growth while the yield of BC/disk was increased by 2.3-fold (2380 mg BC/disk) compared to the conventional HS medium (Table 1). This could be attributed to the favorable nutritional content of BW in vitamins [5]. In this case the WHC of BC was 2-fold lower than that of the HS-derived BC. While glucose-based hydrolysates from alternative feedstocks have been extensively employed for BC fermentation—such as wheat milling by-products (5.2 g/L BC), confectionery waste (5.7 g/L BC) [14,18], rice and corn-derived starch hydrolysates (2.8 g/L BC after 30 days) [63], and waste beer yeast hydrolysates (up to 7.0 g/L BC following optimized ultrasonic treatment and acid hydrolysis) [64]—the utilization of BW as a feedstock for BC production remains largely unexplored, underscoring the novelty of our approach. Specifically, enzymatic hydrolysates of stale bread led to a BC concentration of 2.1 g/L with *K. xylinus* DSM 2004 [65]. In another study, *Gluconobacter oxydans* MG2021 was grown in BW hydrolysate obtained through dilute-acid hydrolysis of various stale bread types, yielding 8.8–25.0 g BC per 100 g of stale bread [66]. To date, only Zahan et al. [50] have reported BC production using a RDB system with agro-food side streams as fermentation media. In that study, *Acetobacter xylinum* 0416 produced 28.3 g of dry BC after 4 days when cultivated on treated liquid pineapple waste in a 10-L RDB. By leveraging BW, we not only address food waste management but also enhance the feasibility of BC production using low-cost, and readily available raw materials, and thus opening new avenues for both waste valorization and biotechnological innovation.

3.7. Characterization of BC and BNCs

3.7.1. ATR-FTIR analysis

The FTIR spectra of BC (produced using HS-based media and BW enzymatic hydrolysates) and BNCs presented typical cellulose vibrations (Fig. 2a and b). The absorbance band within 2998–3726 cm^{-1} was attributed to -OH stretching vibrations while the band in the range 2689–2998 cm^{-1} to the stretching vibration of -CH located in the cellulose backbone of BC and BNCs [67]. The peaks at 1607 cm^{-1} and 1636 cm^{-1} of BC and the strong peak at 1626 cm^{-1} of BNC3 correspond to

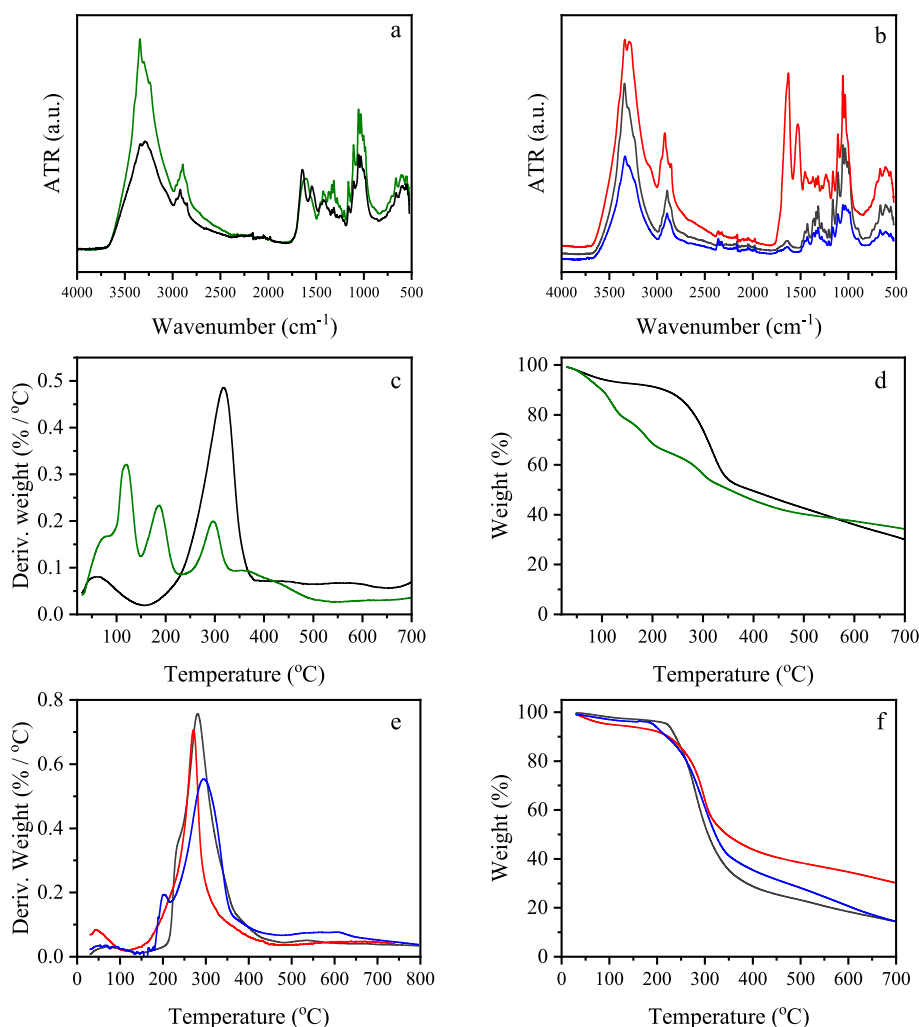


Fig. 2. (a, b) ATR-FTIR spectrum of BC produced in a rotating disk bioreactor (RDB) using glucose-based media (black) and bread waste hydrolysates (green) and BC treated for 24 h with H_2SO_4 (BNC1, dark grey), $\text{H}_2\text{SO}_4/\text{HCl}$ (BNC2, blue), and cellulases (BNC3, red). (c–f) Thermal analysis of BC and treated samples: (c, e) derivative thermogravimetric curves (DTG) and (d, f) thermogravimetric analysis (TGA) of BC produced in the RDB using glucose-based media (black) and bread waste hydrolysates (green), BNC1 (dark grey), BNC2 (blue) and BNC3 (red).

water absorption [13]. Moreover, in the spectrum of BCs (Fig. 2a), the absorption band with a peak at 1315 cm^{-1} reflects the CH_2 rocking vibration at C6 carbon and the peak at 1205 cm^{-1} the C–O–C symmetrical stretching vibration. On the other hand, in the FTIR spectra of BNCs (Fig. 2b), the absorption spectra band at 1428 cm^{-1} is assigned as asymmetric angular deformation and at 898 cm^{-1} as angular deformation of C–H. Asymmetric stretching vibrations of C–O–C glycosidic bonds are reflected in the peak recorded at 1157 cm^{-1} [68]. The stretching of C–OH and C–C–OH bonds in secondary and primary alcohols of BCs and BNCs is responsible for the maxima around 1108 cm^{-1} and within $1055\text{--}981\text{ cm}^{-1}$, respectively. The presence of the H–C–H and O–C–H deformation of cellulose skeletal vibrations of BCs and BNCs is suggested by the peak at 899 cm^{-1} [69].

3.7.2. DLS and electrophoretic light scattering analysis

The size distributions in colloidal suspensions of BCs and BNCs obtained after ex-situ modification were assessed via DLS (Table 3). BC (derived from glucose-based and BW-based media) suspensions presented very similar trimodal size distribution with R_h varying within 65–637 nm. The broad distributions were attributed to the high PDI value of BC dispersions (ca. ~ 0.4), confirming thus the heterogeneity of the mixtures. A bimodal distribution of two peaks, one at 74 nm and the other at 471 nm with PDI = 0.49 was revealed for BNC1 (Table 3). A

Table 3

Physicochemical characterization of bacterial cellulose and treated bacterial cellulose after 24 hour hydrolysis.

Cellulose	R_h (nm)	ζ -potential (mV)	T_{on} ($^{\circ}\text{C}$)	T_f ($^{\circ}\text{C}$)	T_{max} ($^{\circ}\text{C}$)
Glucose-based BC	69 ⁱ , 584 ⁱⁱ , 637 ⁱⁱⁱ	-16.6 ± 6.46^d	280 ^a	349 ^b	317 ^a
BW-based BC	65 ⁱ , 461 ⁱⁱ , 593 ⁱⁱⁱ	-17.0 ± 6.46^d	279 ^a	320 ^d	295 ^b
BNC1	74 ⁱ , 471 ⁱⁱ	-34.7 ± 4.15^a	247 ^b	334 ^c	281 ^{bc}
BNC2	60 ⁱ , 387 ⁱⁱ , 2969 ⁱⁱⁱ	-27.5 ± 3.79^c	239 ^b	345 ^{bc}	294 ^b
BNC3	127 ⁱ , 981 ⁱⁱ	-30.5 ± 4.81^b	238 ^b	373 ^a	271 ^c

Bacterial cellulose (BC) nanostructures obtained after BC hydrolysis with H_2SO_4 (BNC1), mixtures of $\text{H}_2\text{SO}_4\text{-HCl}$ (BNC2) and commercial cellulases (BNC3). The hydrodynamic radius (R_h) values are obtained with a 5 % error.

T_{on} = onset decomposition temperature; T_f = final decomposition temperature, T_{max} = maximum decomposition temperature.

Different superscript letters within same column indicate statistically significant differences ($p < 0.05$).

ⁱ Values correspond to the first peak.

ⁱⁱ Second peak.

ⁱⁱⁱ Third peak detected in DLS diffractogram (not presented).

similar peak distribution at 127 nm and 981 nm (PDI = 0.40) was detected for BNC3. On the other hand, BNC2 demonstrated a trimodal size distribution with average particle sizes of 60 nm, 387 nm and 2969 nm and PDI = 0.49. The size distributions analyzed through CONTIN analysis are weighted by scattered intensity, and the mass of the scattering particles in solution significantly influences the scattered intensity. Hence, the number of smaller-in-size colloidal nanostructures is potentially higher than that of the larger ones. Zhai et al. [70] detected BC and BNC suspensions (produced by HCl hydrolysis for 4 h) of particle sizes at 590 nm with PDI = 0.37 and 221 nm with PDI = 0.18, respectively. Rollini et al. [71] identified polydisperse bimodal size distribution of BNC after 65 % w/w H₂SO₄ hydrolysis in which the strongest peak centered at around 240 nm and the weakest peak at 1030 nm. Accordingly, Singhsa et al. [72] prepared BNCs using 65 % w/w H₂SO₄ and particle sizes within 187–296 nm were revealed. Bimodal size distributions of BNC obtained after acid hydrolysis were detected by Efthymiou et al. [14]. In particular, average particle sizes of 63 nm and 436 nm were monitored for BNC treated with H₂SO₄ (24 h) and 84 nm and 862 nm for BNC hydrolyzed with mixture of H₂SO₄-HCl (24 h). Natsia et al. [18] identified quite comparable bimodal distributions of BNC after 24 h of H₂SO₄ hydrolysis with two peaks at 72 nm and 931 nm.

The ζ -potential values were determined within -16.6 mV to -34.7 mV (Table 3). The absolute ζ -potential values of 15–30 mV suggest that the nanocolloidal systems are at the delicate dispersion/suspension threshold while the values of 30–40 mV suggest moderate stability of systems [73]. The highly negative surface charge of BNC1 and BNC2 is associated with the conjugated sulfate groups ($-\text{OSO}_3^-$) that resulted from the esterification of the hydroxyl groups on the cellulose surface [68]. BNCs treated with HCl present low-density surface charges or a surface charge that is undetectable compared to those treated with H₂SO₄ [74]. On the other hand, the sulfonation of the BNC surface with H₂SO₄ results in a larger negative surface charge [68]. Since there is no HCl interaction with the hydroxyl groups, BNCs treated with a H₂SO₄-HCl mixture have a lower effective charge than BC treated with H₂SO₄. Vasconcelos et al. [68] reported surface charges of -33.6 mV and -36.3 mV for BNC after 60 and 120 min of H₂SO₄ hydrolysis. Moreover, Efthymiou et al. [14] determined ζ -potential values of -32.2 mV and -28.0 for BNC obtained after 24 h H₂SO₄-assisted and H₂SO₄:HCl-assisted hydrolysis, respectively.

3.7.3. Thermal profile

BC produced from glucose-based and BW-based media presented very similar mass-loss profile with BNCs with three different events being identified (Fig. 2c–f). The first event (<150 °C) was attributed to the evaporation of remaining water event and volatile molecules that may appear in the cellulosic matrix. The second event (200–400 °C), that was related to cellulose degradation, including dehydration, breakdown, and depolymerization of the glycoside units, dominated. Oxidation and decomposition of carbon residues occurred during the last event with temperature values up to 600 °C [18]. Vasconcelos et al. [68] reported similar mass-loss profiles for BC and BNC obtained after different conditions of acid hydrolysis. In this study, in the case of BC produced from BW hydrolysates, the first and last event related to water evaporation and cellulose degradation respectively, were also confirmed as aforementioned. An extra event that was detected within 150–230 °C may be attributed to the presence of BW residues in the cellulosic material. These residues may contain starch and low molecular weight compounds which are less thermally stable than cellulose and start to decompose in this temperature range [75].

The decomposition temperature, which serves as an indicator of thermal stability, is influenced by several structural factors, including molecular weight, crystallinity, and fiber alignment, all of which affect BC chain packing and thermal resistance. Variations in this temperature are often linked to differences in the production process (e.g., process parameters, microbial strain, and culture media), purification methods,

and material modifications [56]. In this study, both BC samples exhibited similar onset decomposition temperature (T_{on}) but the maximum decomposition temperature (T_{max}) of BC produced from BW hydrolysates decreased by 6.9 % compared to that derived from commercial fermentation media (317 °C). This decrease may suggest that, despite the 0.22 μm filtration step used to sterilize the BW enzymatic hydrolysates, trace impurities may still be present, influencing the hierarchical assembly of BC fibers. Media impurities can interfere with cellulose biosynthesis and self-assembly, leading to a less organized, lower-crystallinity BC network and ultimately reducing its thermal resistance [76]. This aligns with findings reported by Vasquez et al. [77] who reported a similar decrease in T_{max} and crystallinity for BC produced from biodiesel-derived glycerol and cane bagasse, compared to BC from commercial glucose-based media. To add, heat sterilization of complex fermentation media may induce partial coagulation or flocculation of certain components, such as polyphenols, proteins and metal ions that may be contained in them [46]. Such interactions may disrupt the alignment of cellulose microfibrils, leading to structural irregularities and reduced crystallinity, which, in turn, compromises the thermal stability of the material. High crystallinity values enhance thermal resistance due to the stronger intermolecular hydrogen bonding and denser molecular packing, which restrict polymer chain mobility and delays thermal degradation [78]. Slightly higher T_{max} values compared to our study were reported by Andritsou et al. [69] for BC produced from citrus peels (315 °C), while Vasconcelos et al. [68] and Natsia et al. [18] reported $T_{\text{max}} = 335\text{--}338$ °C for nata de coco and BC produced from wheat milling hydrolysates respectively.

In the case of BNCs, T_{on} varied within 238–247 °C while T_{max} values were lower compared to BC samples (Table 3). The presence of sulfate groups ($-\text{OSO}_3^-$) on the BNC surface during hydrolysis reactions with H₂SO₄ promotes structures with lower thermal stability [18]. Vasconcelos et al. [68] suggested that T_{on} of H₂SO₄-treated BC significantly decreased (218–164 °C) when acid concentrations higher than 50 % were used while the T_{on} of H₂SO₄-HCl treated BC was quite higher (263 °C) than all H₂SO₄-treated BC samples. In this study, the contrary tendency was observed with non-considerable differences.

The ash content in the residual mass of the TG curves was 20 % and 30 % for BC produced with glucose-based media and BW hydrolysates respectively. The residual mass of hydrolyzed BNCs in the TGA presented a low percentage of ashes (10–11 %) for BNC produced by the hydrolysis with H₂SO₄ and H₂SO₄/HCl mix when compared to the enzymatic, which has an ash content of approximately 25 %.

3.7.4. Transmission electron microscopy

The morphology of BNC suspensions was observed by TEM imaging, as presented in Fig. 3. Both H₂SO₄ (Fig. 3ai) and H₂SO₄/HCl (Fig. 3bi) assisted hydrolyses displayed BNC samples with typical rodlike/needlelike nanostructure with width dimensions ranging 33.1 ± 18.2 nm and 24.8 ± 14.2 nm respectively (Fig. 3a, b). It was observed that BNC samples that underwent H₂SO₄-assisted hydrolysis were more homogeneous in size compared to the BNC sample occurring upon H₂SO₄/HCl assisted hydrolysis. This may be attributed to greater electrostatic repulsion due to the higher presence of sulfate groups on the surface among nanostructures within the aqueous suspension [72]. In addition, it has been reported that cellulosic samples treated with strong acids are producing disoriented regions along the cellulose fibrils, therefore sorter nanocrystals [79]. BNC occurring upon enzymatic assisted hydrolysis (Fig. 3ci) resulted in flat ribbons of 56.4 ± 26.3 nm width (Fig. 3c) with bundle of ribbons present in the sample. Overall, it has been shown that the morphology of enzymatically hydrolyzed BC is different and strongly depends on the enzyme/BC ratio. According to a previous study, progressive fibril thinning was observed when increasing the enzyme (cellulase) concentration, with individual nanocrystals as thin as 6 nm, while at the same time large particles were present even for the enzyme-richest mixtures, resulting in high polydispersity of BC-derived nanoparticles [17]. Moreover, independently of the kind of BC hydrolysis

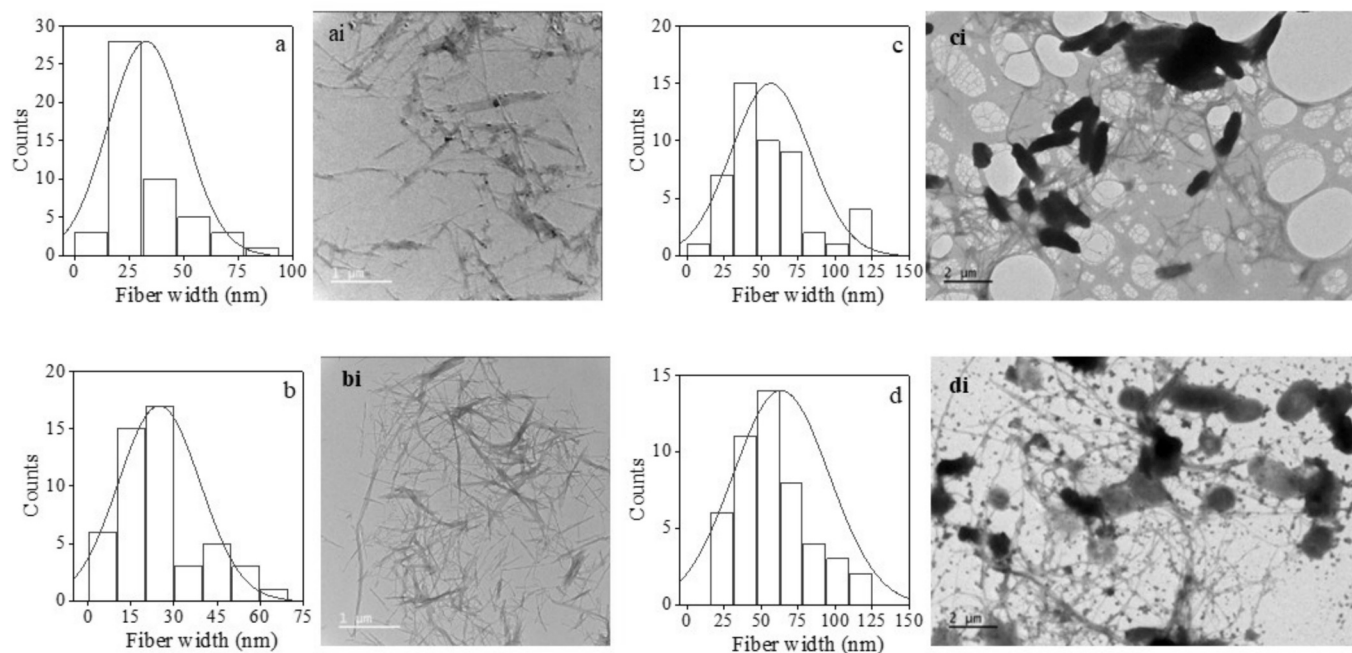


Fig. 3. Transmission electron microscopy of bacterial cellulose from bread waste enzymatic hydrolysates treated (24 h) with H_2SO_4 (BNC1, ai), H_2SO_4/HCl (BNC2, bi), cellulases (BNC3, ci), and untreated (di) and respective fiber diameter distributions (a, b, c, d).

technique, the duration of hydrolysis also plays a critical role on BC nanostructures size. For example, it has been reported that increasing hydrolysis time results in decreasing BC nanowhiskers length [80]. TEM image of BC that has not been subjected to any treatment (Fig. 3di) presents the typical interconnected fibrillar network of BC (width of 63.5 ± 32.2) (Fig. 3d), along with some bacterial cells and media residues/impurities.

4. Conclusions

This study presented the design/manufacture of a novel RDB with magnetic coupling transmission for efficient BC production. Key findings showed that variations in disk submersion, spacing, surface roughness, and rotation speed affected BC production, while aeration significantly boosted BC yields. Substituting commercial glucose with BW enzymatic hydrolysates increased BC production 2.3-folds (2380 mg/disk). The property evaluation highlighted that fermentation media and hydrolysis methods (acid- and enzymatic-assisted hydrolysis) significantly affected the structural, thermal, and morphological properties of the biopolymer. Overall, this study offers insights into the potential of the RDB to achieve scalable BC production using waste-resources. Also, the importance of coupling fermentation and hydrolysis conditions to customize properties for bio-based product development was underscored. By leveraging sustainable fermentation substrates and fine-tuning processing methods, the production of biopolymers can contribute to innovations in environmental sustainability, and circular bioeconomy paving the way for high-performance bio-based materials.

CRedit authorship contribution statement

Sotirios Pilafidis: Writing – original draft, Software, Methodology, Investigation, Formal analysis. **Antiopi Vardaxi:** Writing – original draft, Software, Methodology, Formal analysis. **Konstantina Kourmentza:** Writing – original draft, Methodology. **Stergios Pispas:** Supervision. **Maria Dimopoulou:** Methodology. **Erminta Tsouko:** Writing – review & editing, Writing – original draft, Validation, Supervision, Software, Project administration, Funding acquisition, Data curation, Conceptualization.

Declaration of competing interest

The authors declare that they have no known competing financial interests or personal relationships that could have appeared to influence the work reported in this paper.

Acknowledgements

The authors acknowledge funding of this work by the Hellenic Foundation for Research and Innovation (H.F.R.I.) under the “3rd Call for H.F.R.I. Research Projects to support Post-Doctoral Researchers” (Project Number: 7664). The authors would also like to thank Steve Kalligeros for his guidance and assistance with the design and construction of the RDB.

Data availability

Data will be made available on request.

References

- [1] K. Richardson, W. Steffen, W. Lucht, J. Bendtsen, S.E. Cornell, J.F. Donges, M. Driike, I. Fetzer, G. Bala, W. von Bloh, G. Feulner, S. Fiedler, D. Gerten, T. Gleeson, M. Hofmann, W. Huiskamp, M. Kumm, C. Mohan, D. Nogués-Bravo, S. Petri, M. Porkka, S. Rahmstorf, S. Schaphoff, K. Thonicke, A. Tobian, V. Virkki, L. Wang-Erlandsson, L. Weber, J. Rockström, Earth beyond six of nine planetary boundaries, *science, Advances* 9 (2023) eadh2458, <https://doi.org/10.1126/sciadv.adh2458>.
- [2] E. Elhacham, L. Ben-Uri, J. Grozovski, Y.M. Bar-On, R. Milo, Global human-made mass exceeds all living biomass, *Nature* 588 (2020) 442–444, <https://doi.org/10.1038/s41586-020-3010-5>.
- [3] S. Tsokri, M. Sarafidou, E. Tsouko, E. Athanasopoulou, A. Vardaxi, S. Pispas, T. Tsironi, A. Koutinas, Efficient pectin recovery from sugar beet pulp as effective bio-based coating for Pacific white shrimp preservation, *Int. J. Biol. Macromol.* 282 (2024) 136754, <https://doi.org/10.1016/j.ijbiomac.2024.136754>.
- [4] V. Kumar, P. Brancoli, V. Narisetty, S. Wallace, D. Charalampopoulos, B. Kumar Dubey, G. Kumar, A. Bhatnagar, S. Kant Bhatia, M.J. Taherzadeh, Bread waste – a potential feedstock for sustainable circular biorefineries, *Bioresour. Technol.* 369 (2023) 128449, <https://doi.org/10.1016/j.biortech.2022.128449>.
- [5] A. Dymchenko, M. Geršl, T. Gregor, Trends in bread waste utilisation, *Trends Food Sci. Technol.* 132 (2023) 93–102, <https://doi.org/10.1016/j.tifs.2023.01.004>.
- [6] M. Alexandri, J. Blanco-Catalá, R. Schneider, X. Turon, J. Venus, High L(+)-lactic acid productivity in continuous fermentations using bakery waste and lucerne

- green juice as renewable substrates, *Bioresour. Technol.* 316 (2020) 123949, <https://doi.org/10.1016/j.biortech.2020.123949>.
- [7] S. Maina, R. Schneider, M. Alexandri, H. Papapostolou, G.-J. Nychas, A. Koutinas, J. Venus, Volumetric oxygen transfer coefficient as fermentation control parameter to manipulate the production of either acetoin or D-2,3-butanediol using bakery waste, *Bioresour. Technol.* 335 (2021) 125155, <https://doi.org/10.1016/j.biortech.2021.125155>.
- [8] D. Selianitis, M.-N. Efthymiou, E. Tsouko, A. Papagiannopoulos, A. Koutinas, S. Pispas, Nanocellulose production from different sources and their self-assembly in composite materials, in: A. Barhoum (Ed.), *Handbook of nanocelluloses*, Springer International Publishing, Cham, 2021, pp. 1–32, <https://doi.org/10.1007/978-3-030-62976-2-7-1>.
- [9] L. Xiao, L. Webb, X. Lu, The role of bacterial cellulose in cellular agriculture, in: E. D.G. Fraser, D.L. Kaplan, L. Newman, R.Y. Yada (Eds.), *Cellular agriculture*, Academic Press, 2024, pp. 311–322, <https://doi.org/10.1016/B978-0-443-18767-4.00018-4>.
- [10] J. Wang, J. Tavakoli, Y. Tang, Bacterial cellulose production, properties and applications with different culture methods – a review, *Carbohydr. Polym.* 219 (2019) 63–76, <https://doi.org/10.1016/j.carbpol.2019.05.008>.
- [11] P.R. Chawla, I.B. Bajaj, S.A. Surve, R.S. Singhal, *Microbial cellulose: fermentative production and applications*, *Food Technol. Biotechnol.* 47 (2009).
- [12] M. Liu, S. Li, Y. Xie, S. Jia, Y. Hou, C. Zhong, Enhanced bacterial cellulose production by *Gluconacetobacter xylinus* via expression of *Vitreoscilla* hemoglobin and oxygen tension regulation, *Appl. Microbiol. Biotechnol.* 102 (2018) 1155–1165, <https://doi.org/10.1007/s00253-017-8680-z>.
- [13] V.S. Soeiro, L.L. Tundisi, L.C.L. Novaes, P.G. Mazzola, N. Aranha, D. Grotto, J.M. O. Júnior, D. Komatsu, F.M.P. Gama, M.V. Chaud, A.F. Jozala, Production of bacterial cellulose nanocrystals via enzymatic hydrolysis and evaluation of their coating on alginate particles formed by ionotropic gelation, *Carbohydrate Polymer Technologies and Applications* 2 (2021) 100155, <https://doi.org/10.1016/j.carpta.2021.100155>.
- [14] M.-N. Efthymiou, E. Tsouko, C. Pateraki, A. Papagiannopoulos, P. Tzamalís, S. Pispas, K. Bethanis, I. Mantala, A. Koutinas, Property evaluation of bacterial cellulose nanostructures produced from confectionery wastes, *Biochem. Eng. J.* 186 (2022) 108575, <https://doi.org/10.1016/j.bej.2022.108575>.
- [15] E. Tsouko, S. Pilafidis, M. Dimopoulou, K. Kourmentza, D. Sarris, Bioconversion of underutilized brewing by-products into bacterial cellulose by a newly isolated *Komagataeibacter rhaeticus* strain: a preliminary evaluation of the bioprocess environmental impact, *Bioresour. Technol.* 387 (2023) 129667, <https://doi.org/10.1016/j.biortech.2023.129667>.
- [16] S. Hestrin, M. Schramm, Synthesis of cellulose by *Acetobacter xylinum*. 2. Preparation of freeze-dried cells capable of polymerizing glucose to cellulose, *Biochem. J.* 58 (1954) 345.
- [17] C. Rovera, M. Ghaani, N. Santo, S. Trabattoni, R.T. Olsson, D. Romano, S. Farris, Enzymatic hydrolysis in the green production of bacterial cellulose nanocrystals, *ACS Sustain. Chem. Eng.* 6 (2018) 7725–7734, <https://doi.org/10.1021/acssuschemeng.8b00600>.
- [18] A. Natsia, E. Tsouko, C. Pateraki, M.-N. Efthymiou, A. Papagiannopoulos, D. Selianitis, S. Pispas, K. Bethanis, A. Koutinas, Valorization of wheat milling by-products into bacterial nanocellulose via ex-situ modification following circular economy principles, *Sustain. Chem. Pharm.* 29 (2022) 100832, <https://doi.org/10.1016/j.scp.2022.100832>.
- [19] G.L. Miller, Use of dinitrosalicylic acid reagent for determination of reducing sugar, *Anal. Chem.* 31 (1959) 426–428.
- [20] S. Lie, The EBC-NINHYDRIN method for determination of free ALPHA amino nitrogen, *J. Inst. Brewing* 79 (1973) 37–41, <https://doi.org/10.1002/j.2050-0416.1973.tb03495.x>.
- [21] W. Horwitz, *Official methods of analysis of AOAC International*, in: William Horwitz (Ed.), *Agricultural Chemicals, Contaminants, Drugs Vol. I*, AOAC International, Gaithersburg (Maryland), 1997, p. 2010.
- [22] A. International, *Approved Methods of Analysis*, AACC International: St. Paul, MN, 2010.
- [23] F. Hassard, J. Biddle, E. Cartmell, B. Jefferson, S. Tyrrel, T. Stephenson, Rotating biological contactors for wastewater treatment – a review, *Process Saf. Environ. Prot.* 94 (2015) 285–306, <https://doi.org/10.1016/j.psep.2014.07.003>.
- [24] A.W. Patwardhan, Rotating biological contactors: a review, *Ind. Eng. Chem. Res.* 42 (2003) 2035–2051, <https://doi.org/10.1021/ie0200104>.
- [25] M. Hackbarth, J. Gescher, H. Horn, J.E. Reiner, A scalable, rotating disc bioelectrochemical reactor (RDBER) suitable for the cultivation of both cathodic and anodic biofilms, *Bioresour. Technol. Rep.* 21 (2023) 101357, <https://doi.org/10.1016/j.biteb.2023.101357>.
- [26] L. Di Palma, N. Verdone, The effect of disk rotational speed on oxygen transfer in rotating biological contactors, *Bioresour. Technol.* 100 (2009) 1467–1470, <https://doi.org/10.1016/j.biortech.2008.07.058>.
- [27] L. Jäger, S. Scholl, Experimental characterization and mixing modeling of a horizontally rotating disc reactor, *Chem. Eng. Sci.* 280 (2023) 118995, <https://doi.org/10.1016/j.ces.2023.118995>.
- [28] L. de Porto Souza Vannbergh, L. Wedderhoff Herrmann, R. de Oliveira Penha, A. F. de Murawski Mello, W.J. Martínez-Burgos, A.I. Magalhães Junior, P.C. de Souza Kireny, J.C. de Carvalho, C.R. Soccol, Engineering aspects for scale-up of bioreactors, in: R. Sirohi, A. Pandey, M.J. Taherzadeh, C. Larroche (Eds.), *Current Developments in Biotechnology and Bioengineering*, Elsevier, 2022, pp. 59–85, <https://doi.org/10.1016/B978-0-323-91167-2.00002-2>.
- [29] S. Waqas, N.Y. Harun, N.S. Sambudi, M.R. Bilad, K.J. Abioye, A. Ali, A. Abdulrahman, A review of rotating biological contactors for wastewater treatment, *Water* 15 (2023) 1913, <https://doi.org/10.3390/w15101913>.
- [30] M.A. Cruz, O. Flor-Unda, A. Avila, M.D. Garcia, L. Cerda-Mejía, Advances in bacterial cellulose production: a scoping review, *Coatings* 14 (2024) 1401, <https://doi.org/10.3390/coatings14111401>.
- [31] A. Soleimani, S. Hamed, V. Babeiour, M. Rouhi, Design, construction and optimization a flexible bench-scale rotating biological contactor (RBC) for enhanced production of bacterial cellulose by *Acetobacter xylinum*, *Bioprocess Biosyst. Eng.* 44 (2021) 1071–1080, <https://doi.org/10.1007/s00449-021-02510-0>.
- [32] M. Konuhova, E. Kamolins, S. Orlova, A. Suleiko, R. Otankis, Optimisation of permanent magnets of bioreactor magnetic coupling while preserving their efficiency, *Latv. J. Phys. Tech. Sci.* 56 (2019) 38–48, <https://doi.org/10.2478/lpts-2019-0023>.
- [33] A. Suleiko, J. Vanags, M. Konuhova, K. Dubencovs, O. Grigs, The application of novel magnetically coupled mixer drives in bioreactors of up to 15 m³, *Biochem. Eng. J.* 154 (2020) 107464, <https://doi.org/10.1016/j.bej.2019.107464>.
- [34] J. Vanags, U. Viesturs, I. Fort, Mixing intensity studies in a pilot plant stirred bioreactor with an electromagnetic drive, *Biochem. Eng. J.* 3 (1999) 25–33, [https://doi.org/10.1016/S1369-703X\(98\)00042-4](https://doi.org/10.1016/S1369-703X(98)00042-4).
- [35] C.K. Tan, M.J. Davies, D.K. McCluskey, I.R. Munro, M.C. Nweke, M.C. Tracey, N. Szita, Electromagnetic stirring in a microbioreactor with non-conventional chamber morphology and implementation of multiplexed mixing, *J. Chem. Technol. Biotechnol.* 90 (2015) 1927–1936, <https://doi.org/10.1002/jctb.4762>.
- [36] C. Schirmer, R.W. Maschke, R. Pörtner, D. Eibl, An overview of drive systems and sealing types in stirred bioreactors used in biotechnological processes, *Appl. Microbiol. Biotechnol.* 105 (2021) 2225–2242, <https://doi.org/10.1007/s00253-021-11180-7>.
- [37] S.-P. Lin, S.-C. Hsieh, K.-I. Chen, A. Demirci, K.-C. Cheng, Semi-continuous bacterial cellulose production in a rotating disk bioreactor and its materials properties analysis, *Cellulose* 21 (2014) 835–844, <https://doi.org/10.1007/s10570-013-0136-8>.
- [38] N. Pa'e, K.A. Zahan, I.I. Muhamad, Production of biopolymer from *Acetobacter xylinum* using different fermentation methods, *Int. J. Eng.* 11 (2011).
- [39] N. Cohen, E. Sicher, C. Ayala-Garcia, I.M. Sanchez-Fayos, L. Conterno, S. Ugur Yavuz, Innocent bioreactor: an open-source development to produce biomaterials for food and packaging based on fermentation processes, *Fermentation* 9 (2023) 915, <https://doi.org/10.3390/fermentation9100915>.
- [40] Y.-J. Kim, J.-N. Kim, Y.-J. Wee, D.-H. Park, H.-W. Ryu, Bacterial cellulose production by *Gluconacetobacter* sp. PKY5 in a rotary biofilm contactor, *Appl. Biochem. Biotechnol.* 137–140 (2007) 529–537, <https://doi.org/10.1007/s12010-007-9077-8>.
- [41] C. Sharma, N.K. Bhardwaj, P. Pathak, Rotary disc bioreactor-based approach for bacterial nanocellulose production using *Gluconacetobacter xylinus* NCIM 2526 strain, *Cellulose* 29 (2022) 7177–7191, <https://doi.org/10.1007/s10570-022-04739-8>.
- [42] K. Jin, C. Jin, Y. Wu, Synthetic biology-powered microbial co-culture strategy and application of bacterial cellulose-based composite materials, *Carbohydr. Polym.* 283 (2022) 119171, <https://doi.org/10.1016/j.carbpol.2022.119171>.
- [43] H.R. Bungay, G.C. Serafica, Production of Microbial Cellulose Using a Rotating Disk Film Bioreactor, US955326A. <https://patents.google.com/patent/US955326A/en>, 1999. (Accessed 13 February 2024).
- [44] W. Czaja, D. Romanovicz, R. Malcolm Brown, Structural investigations of microbial cellulose produced in stationary and agitated culture, *Cellulose* 11 (2004) 403–411, <https://doi.org/10.1023/B:CELL.0000046412.11983.61>.
- [45] A. Pandit, R. Kumar, A review on production, characterization and application of bacterial cellulose and its biocomposites, *J. Polym. Environ.* 29 (2021) 2738–2755, <https://doi.org/10.1007/s10924-021-02079-5>.
- [46] E. Tsouko, S. Pilafidis, K. Kourmentza, H.I. Gomes, G. Sarris, P. Koralli, A. Papagiannopoulos, S. Pispas, D. Sarris, A sustainable bioprocess to produce bacterial cellulose (BC) using waste streams from wine distilleries and the biodesign industry: evaluation of BC for adsorption of phenolic compounds, dyes and metals, *Biotechnol. Biofuels* 17 (2024) 40, <https://doi.org/10.1186/s13068-024-02488-3>.
- [47] K. Anguluri, S. La China, M. Brugnoli, S. Cassanelli, M. Gullo, Better under stress: improving bacterial cellulose production by *Komagataeibacter xylinus* K2G30 (UMCC 2756) using adaptive laboratory evolution, *Front. Microbiol.* 13 (2022) 994097, <https://doi.org/10.3389/fmicb.2022.994097>.
- [48] D. Lahiri, M. Nag, B. Dutta, A. Dey, T. Sarkar, S. Pati, H.A. Edinur, Z. Abdul Kari, N. H. Mohd Noor, R.R. Ray, Bacterial cellulose: production, characterization, and application as antimicrobial agent, *IJMS* 22 (2021) 12984, <https://doi.org/10.3390/ijms222312984>.
- [49] C. Zhong, Industrial-scale production and applications of bacterial cellulose, *Front. Bioeng. Biotechnol.* 8 (2020), <https://doi.org/10.3389/fbioe.2020.605374>.
- [50] K.A. Zahan, N. Pa'e, I.I. Muhamad, Process parameters for fermentation in a rotary disc reactor for optimum microbial cellulose production using response surface methodology, *Bioresour. J.* 9 (2014).
- [51] E.J. Vandamme, S. De Baets, A. Vanbaelen, K. Joris, P. De Wulf, Improved production of bacterial cellulose and its application potential, *Polym. Degrad. Stab.* 59 (1998) 93–99, [https://doi.org/10.1016/S0141-3910\(97\)00185-7](https://doi.org/10.1016/S0141-3910(97)00185-7).
- [52] F. Yoshinaga, N. Tonouchi, K. Watanabe, Research Progress in production of bacterial cellulose by aeration and agitation culture and its application as a new industrial material, *Biosci. Biotechnol. Biochem.* 61 (1997) 219–224, <https://doi.org/10.1271/bbb.61.219>.
- [53] S.-P. Lin, C.-T. Liu, K.-D. Hsu, Y.-T. Hung, T.-Y. Shih, K.-C. Cheng, Production of bacterial cellulose with various additives in a PCS rotating disk bioreactor and its material property analysis, *Cellulose* 23 (2016) 367–377.
- [54] E. Tsouko, S. Maina, D. Ladakis, I.K. Kookos, A. Koutinas, Integrated biorefinery development for the extraction of value-added components and bacterial cellulose

- production from orange peel waste streams, *Renew. Energy* 160 (2020) 944–954, <https://doi.org/10.1016/j.renene.2020.05.108>.
- [55] S. Mishra, P.K. Singh, R. Pattnaik, S. Kumar, S.K. Ojha, H. Srichandan, P.K. Parhi, R.K. Jyothi, P.K. Sarangi, Biochemistry, synthesis, and applications of bacterial cellulose: a review, *Front. Bioeng. Biotechnol.* 10 (2022) 780409, <https://doi.org/10.3389/fbioe.2022.780409>.
- [56] V. Girard, J. Chaussé, P. Vermette, Bacterial cellulose: A comprehensive review, *J of Applied Polymer Sci* 141 (2024) e55163, <https://doi.org/10.1002/app.55163>.
- [57] F.G. Blanco Parte, S.P. Santoso, C.-C. Chou, V. Verma, H.-T. Wang, S. Ismadji, K.-C. Cheng, Current progress on the production, modification, and applications of bacterial cellulose, *Crit. Rev. Biotechnol.* 40 (2020) 397–414, <https://doi.org/10.1080/07388551.2020.1713721>.
- [58] Y. Chao, Y. Sugano, M. Shoda, Bacterial cellulose production under oxygen-enriched air at different fructose concentrations in a 50-liter, internal-loop airlift reactor, *Appl. Microbiol. Biotechnol.* 55 (2001) 673–679.
- [59] M. Liu, C. Zhong, X.-Y. Wu, Y.-Q. Wei, T. Bo, P.-P. Han, S.-R. Jia, Metabolomic profiling coupled with metabolic network reveals differences in *Gluconacetobacter xylinus* from static and agitated cultures, *Biochem. Eng. J.* 101 (2015) 85–98, <https://doi.org/10.1016/j.bej.2015.05.002>.
- [60] A.Y. Zhang, Z. Sun, C.C.J. Leung, W. Han, K.Y. Lau, M. Li, C.S.K. Lin, Valorisation of bakery waste for succinic acid production, *Green Chem.* 15 (2013) 690–695, <https://doi.org/10.1039/C2GC36518A>.
- [61] T. Sigiienza-Andrés, V. Pando, M. Gómez, J.M. Rodríguez-Nogales, Optimization of a simultaneous enzymatic hydrolysis to obtain a high-glucose slurry from bread waste, *Foods* 11 (2022) 1793, <https://doi.org/10.3390/foods11121793>.
- [62] A. Sükrü Demirci, I. Palabiyik, T. Gümitis, Ş. Özalp, Waste bread as a biomass source: optimization of enzymatic hydrolysis and relation between rheological behavior and glucose yield, *Waste Biomass Valor* 8 (2017) 775–782, <https://doi.org/10.1007/s12649-016-9601-6>.
- [63] K.C. de Souza, G.R. dos Santos, F.C. Trindade, A.F. de S. Costa, Y.M. de Almeida, L. A. Sarubbo, G.M. Vinhas, Production of bacterial cellulose biopolymers in media containing rice and corn hydrolysate as carbon sources, *Polym. Polym. Compos.* 29 (9_suppl) (2021) S1466–S1474, <https://doi.org/10.1177/09673911211059706>.
- [64] D. Lin, P. Lopez-Sanchez, R. Li, Z. Li, Production of bacterial cellulose by *Gluconacetobacter hansenii* CGMCC 3917 using only waste beer yeast as nutrient source, *Bioresour. Technol.* 151 (2014) 113–119, <https://doi.org/10.1016/j.biortech.2013.10.052>.
- [65] A. Esmail, M. Morais, U.D. Yilmazer, L.A. Neves, F. Freitas, Bacterial cellulose production through the valorization of waste apple pulp and stale bread, *Biomass Conv. Bioref.* (2024), <https://doi.org/10.1007/s13399-024-06281-y>.
- [66] M. Güzel, Valorisation of bread wastes via the bacterial cellulose production, *Biomass Conv. Bioref.* 15 (2025) 4777–4790, <https://doi.org/10.1007/s13399-024-05662-7>.
- [67] I.W. Arnata, S. Suprihatin, F. Fahma, N. Richana, T.C. Sunarti, Cationic modification of nanocrystalline cellulose from sago fronds, *Cellulose* 27 (2020) 3121–3141, <https://doi.org/10.1007/s10570-019-02955-3>.
- [68] N.F. Vasconcelos, J.P.A. Feitosa, F.M.P. da Gama, J.P.S. Morais, F.K. Andrade, M. de S.M. de Souza Filho, M. de F. Rosa, Bacterial cellulose nanocrystals produced under different hydrolysis conditions: properties and morphological features, *Carbohydr. Polym.* 155 (2017) 425–431, <https://doi.org/10.1016/j.carbpol.2016.08.090>.
- [69] V. Andritsou, E.M. de Melo, E. Tsouko, D. Ladakis, S. Maragkoudaki, A.A. Koutinas, A.S. Matharu, Synthesis and characterization of bacterial cellulose from citrus-based sustainable resources, *ACS Omega* 3 (2018) 10365–10373, <https://doi.org/10.1021/acsomega.8b01315>.
- [70] X. Zhai, D. Lin, W. Li, X. Yang, Improved characterization of nanofibers from bacterial cellulose and its potential application in fresh-cut apples, *Int. J. Biol. Macromol.* 149 (2020) 178–186, <https://doi.org/10.1016/j.ijbiomac.2020.01.230>.
- [71] M. Rollini, A. Musatti, D. Cavicchioli, D. Bussini, S. Farris, C. Rovera, D. Romano, S. De Benedetti, A. Barbiroli, From cheese whey permeate to Sakacin-A/bacterial cellulose nanocrystal conjugates for antimicrobial food packaging applications: a circular economy case study, *Sci. Rep.* 10 (2020) 21358.
- [72] P. Singhsa, R. Narain, H. Manusiya, Bacterial cellulose nanocrystals (BCNC) preparation and characterization from three bacterial cellulose sources and development of functionalized BCNCs as nucleic acid delivery systems, *ACS Appl. Nano Mater.* 1 (2018) 209–221, <https://doi.org/10.1021/acsnanm.7b00105>.
- [73] N. Pippa, N. Pippa, S. Pispas, C. Demetzos, Physico-chemical characterization and basic research principles of advanced drug delivery nanosystems, in: *Intelligent Nanomaterials*, 2016, pp. 107–125, <https://doi.org/10.1002/9781119242628.ch5>.
- [74] D.K. Arserim-Uçar, F. Korel, L. Liu, K.L. Yam, Characterization of bacterial cellulose nanocrystals: effect of acid treatments and neutralization, *Food Chem.* 336 (2021) 127597, <https://doi.org/10.1016/j.foodchem.2020.127597>.
- [75] S. Rojas-Lema, K. Nilsson, J. Trifol, M. Langton, J. Gomez-Caturla, R. Balart, D. Garcia-Garcia, R. Moriana, Faba bean protein films reinforced with cellulose nanocrystals as edible food packaging material, *Food Hydrocoll.* 121 (2021) 107019, <https://doi.org/10.1016/j.foodhyd.2021.107019>.
- [76] Z. Hussain, W. Sajjad, T. Khan, F. Wahid, Production of bacterial cellulose from industrial wastes: a review, *Cellulose* 26 (2019) 2895–2911, <https://doi.org/10.1007/s10570-019-02307-1>.
- [77] A. Vazquez, M.L. Foresti, P. Cerrutti, M. Galvagno, Bacterial cellulose from simple and low cost production media by *Gluconacetobacter xylinus*, *J. Polym. Environ.* 21 (2013) 545–554, <https://doi.org/10.1007/s10924-012-0541-3>.
- [78] G. Wang, M. Kudo, K. Daicho, S. Harish, B. Xu, C. Shao, Y. Lee, Y. Liao, N. Matsushima, T. Kodama, F. Lundell, L.D. Söderberg, T. Saito, J. Shiomi, Enhanced high thermal conductivity cellulose filaments via hydrodynamic focusing, *Nano Lett.* 22 (2022) 8406–8412, <https://doi.org/10.1021/acs.nanolett.2c02057>.
- [79] M.A.S. Azizi Samir, F. Alloin, A. Dufresne, Review of recent research into cellulosic whiskers, their properties and their application in nanocomposite field, *Biomacromolecules* 6 (2005) 612–626, <https://doi.org/10.1021/bm0493685>.
- [80] M. Martínez-Sanz, A. Lopez-Rubio, J.M. Lagaron, Optimization of the nanofabrication by acid hydrolysis of bacterial cellulose nanowhiskers, *Carbohydr. Polym.* 85 (2011) 228–236, <https://doi.org/10.1016/j.carbpol.2011.02.021>.